Int. J. Electrochem. Sci., 12 **(2017)** 8357 – 8367, doi: 10.20964/2017.09.12

International Journal of
ELECTROCHEMICAL
SCIENCE
www.electrochemsci.org

Preparation of Graphene-Copper Nanocomposite for Electrochemical Determination of Cadmium Ions in Water

Chunjiang Liu[1] *and Changlu Qiao*[2*]

[1] School of economics and management, Chang'an University, Xi'an, Shanxi, 710000, P.R. China
[2] School of Water Conservancy & Architectural Engineering, Shihezi University, Shihezi, Xinjiang 832003, P.R. China
E-mail: qiaochanglu@126.com

Received: 27 February 2017 / *Accepted:* 21 June 2017 / *Published:* 13 August 2017

Films of a graphene/copper composite in a copper matrix were deposited on ITO using an aqueous electrolyte solution containing 0.2 M $CuSO_4$ and a graphene oxide suspension at a low current density. Using a further calefaction of the specimens under a flowing hydrogen atmosphere, graphene oxide was reduced. After this, the detection of cadmium(II) using square-wave voltammetry (SWV) on the Cu-graphene/ITO film was illustrated. This approach utilized ion accumulation on the Cu-graphene/ITO film. The performance of the Cu-graphene/ITO film was optimized by surface modification and changing the operating conditions.

Keywords: Graphene; Copper; Nanocomposite; Cadmium ions; Electrochemical sensor; Water

1. INTRODUCTION

Cadmium has a negative influence on nearly every mechanism in the body, such as the kidneys and the reproductive system. Quantifying trace levels of cadmium has been a challenging issue, and this issue has been known for a long time. Many analytical methods have been used to quantify cadmium. Currently, the quantification of heavy metals at surface and subsurface hazardous waste sites depends on the assembly of discrete liquid specimens for the follow-up analysis with methods, such as atomic absorption spectroscopy (AAS) and inductively coupled plasma mass spectrometry (ICP-MS) [1]. Sensors for the acquisition of real-time ppb levels of heavy metal concentrations would cut down the time and expenses related to the characterization and disposal of hazardous waste sites. The favorable features of metal ion sensors include the specificity for individual metal ions, increased

measurement frequency and accuracy, stability, cost effectiveness and durability of the sensor material. Electrochemical sensors have been found to exhibit the abovementioned features [2].

A variety of materials, such as polymers [3-6], metal [7-10] and metal oxide [11-17] nanoparticles (NPs), and carbon-based substances and their composites [18-20], have been developed to fabricate non-enzymatic sensors. In particular, metal and metal oxide NPs, including Pt [21], Cu [22, 23], CuO [11, 24], and Pd [25] NPs, have aroused significant interest due to their large surface areas, high surface energies, and high electrocatalytic activities in various electrochemical reactions, such as glucose electrooxidation. In general, these NPs are loaded onto an inorganic/organic support to be utilized as electrochemical catalysts. To obtain excellent sensitivity and a low detection limit, it is vital to ensure both even dispersion and unhindered electron transport between the superficial layer of the NPs and electrode. Recently, conductive polymers have attracted much interest since they can be applied as a metal NP stabilizer and a favorable electrocatalyst support due to their outstanding electronic conductivity and multifunctionality [26-29].

Graphene (Gr) is a two-dimensional layer of sp^2-bonded carbon atoms closely packed into a honeycomb lattice. In view of its special features, such as large surface area, excellent electrical conductivity, and large mechanical force, graphene has been commonly used in a variety of fields, including field-effect transistors [30, 31], gas transducers [32, 33], electromechanical sensors/biosensors [34-36], nanoelectronics [37], cells [38, 39], supercapacitors [40] and hydrogen conservation [41]. In addition, graphene can be easily modified through the utilization of strong π-π bonding between its superficial π-orbitals and the π-orbitals of several other flat aromatic molecules. Consequently, several kinds of composite materials between graphene and other substances, such as metal oxides, metals, polymers, and even carbon nanotubes, possessing novel functions have been deemed as promising materials in a variety of fields, including electrochemical sensing.

The aim of this work is to research the effects of the addition of graphene to a Cu matrix on the electrochemical properties. The preparation of graphene composites with copper matrices were accomplished through the electrochemical sedimentation of copper foil in a copper sulfate electrolyte solution and a Cu anode. The obtained Cu-graphene composite specimens underwent tests to determine their electrical transport properties. As a result, we investigated the detection of cadmium cations on the Cu-graphene-modified electrode based on the accumulation course.

2. EXPERIMENTAL

All the substances adopted in the tests were of analytical purity.

A 0.2 M copper sulfate solution was prepared in distilled water. Two pieces of ITO were washed thoroughly with 50% dilute H_2SO_4 and HNO_3. The two pieces of ITO were linked at their ends through a copper wire with a diameter of 1 mm. Both were adopted to serve as the cathode, while the anode was a copper plate (1 mm in thickness and 3 cm × 5 cm in size). For the electrolytic sedimentation, a DC power supply was applied. For the entire deposition, the current was kept at a low level, namely, 0.035 A, and was monitored by the voltage across an electrical resistor of 10 Ω connected in series. At the cathode, the estimated current density was ~1.75 mA/cm^3. The low current

density allowed smooth films with large grain sizes to developed on the ITO. To maintain a homogenous distribution of the electrolyte in the deposition process, a magnetic stirrer was utilized. It was observed that the film growth rate was within the range of 2-3μm/h. The film grew at a constant rate before desired specimen thickness was acquired.

The electrochemical sedimentation of the Cu-graphene composite was accomplished under the same conditions, except that the electrolytic $CuSO_4$ solution contained a GO suspension in distilled water. The GO suspension was fabricated through chemical exfoliation and subsequent sonication. After the deposition, the specimens were prepared for 50 h. When the deposition of each Cu-graphene specimen was accomplished, the GO suspension was refilled. The pH of the solution was nearly 6 by adding 10 cm^3 of 1 M H_2SO_4 to the electrolytic solution. GO has been found to be an amphiphile possessing a large hydrophobic basal plane as well as hydrophilic edges.

The electrolytic Cu and Cu-graphene oxide composite films that were precipitated on ITO were heated under a flowing hydrogen atmosphere with a branched pressure of 20 Torr at 150 °C for 3 hours to give reduce the GO to graphene and then develop the Cu–graphene composites. Calefaction and cooling of the specimens were conducted step by step. Therefore, oxygen evolution and the development of water vapor were reduced on the films. The entire time for hydrogen processing was greater than 6 h for every specimen.

For the detection of Cd ions, the Cu-graphene-modified ITO was soaked in a solution containing 20 ml of cadmium(II) with magnetic stirring at the open circuit potential. Subsequently, the electrode was removed, washed and dried using absorbent paper. After this, the electrode was transported to a 0.2 M KNO_3 solution. In addition, a potential of −1.0 V versus Ag/AgCl was applied for 10 s in the immobile solution. As soon as the reduction time was complete, the second-order derivative voltammogram was performed by applying a single positive potential scan within the range of −1.0 to −0.5 V at 50 mV/s at a scan rate of 1 mV/s, and the step potential, amplitude and duration were 25 mV, 5 mV and 5 s, respectively. All the experiments were carried out at room temperature.

Electrochemical impedance spectroscopy (EIS) measurements were performed before and after the accumulation procedure with a three-electrode setup. The impedance spectra were recorded within the frequency range of 100 to 10 mHz with 10 points per decade at a potential of 0 V after infusion for 30 min for the non-deaerated solutions. A sinusoidal wave with an amplitude of 10 mV was utilized to model the mechanism.

3. RESULTS AND DISCUSSION

The two electrodeposited Cu films on ITO were additionally characterized since the electrodeposited Cu showed diverse electrical resistivity values as well as temperature coefficients of the electrical resistance. To perform the electrical measurements, the specimens were cut into narrower pieces using a diamond saw, but the thicknesses of these specimens were unchanged compared to those of the formed films on ITO. Conductive copper tape with a conductive adhesive on one side was bound to each side of the specimen to enable the transmission of a set current, and the voltage measurements were made through dual internal pins with Signatone equipment. The temperature

coefficient of resistance, TCR = (dR/dT)/R, where R represents the resistance, and T corresponds to the temperature of the specimen, was recorded using a temperature-controlled Dewar and a K-20 temperature controller provided by MMR technology. Under this control, the temperature was maintained at a value within ±0.01 K. The results of the change of resistance at various heating temperatures in the calefaction and cooling process can be seen in Figure 1 for Cu–graphene. Through these three measurements, the slope of the resistance and the TCR at 300 K was determined.

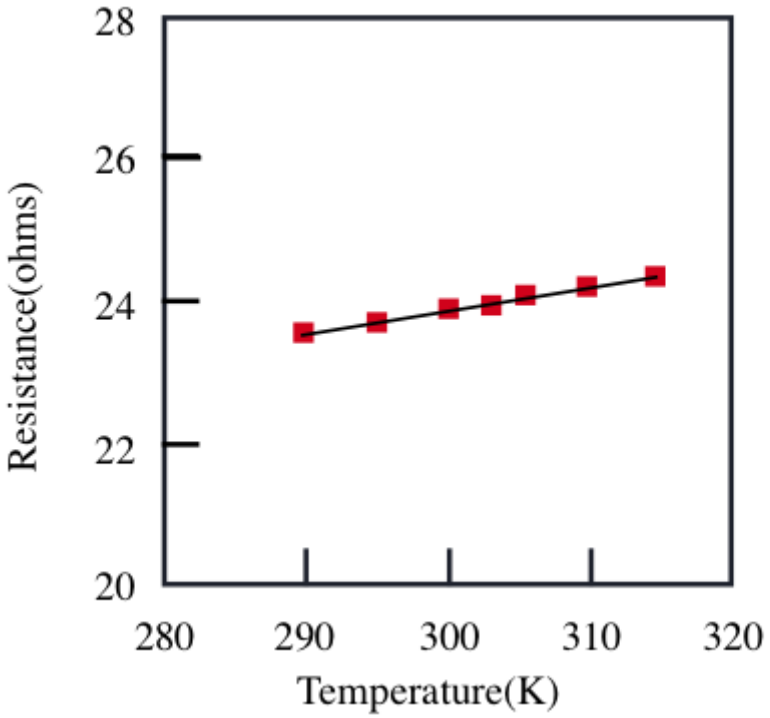

Figure 1. Change of resistance of the Cu–graphene specimen at various temperatures. The red points are representative of the data for the calefaction, while the blue points are representative of the data for the cooling. The straight line was determined by the TCR equation.

X-ray diffraction of the composite specimen prior to hydrogen processing was conducted using Cu $K\alpha$ radiation in a θ–2θ geometry with a Rigaku instrument. As shown in Figure 2, the diffraction pattern is found to have an obvious peak at 2θ = 11.8°, which is related to GO. The diffraction pattern also shows that no peak related to graphite at 2θ = 26.5° appeared. Owing to this, graphite was absent in these specimens. The specimens after hydrogen processing failed to reveal graphene peaks, showing signals consistent with those of the graphite, which was caused by the weak peaks and the small thickness of graphene. In addition, the carbon X-ray scattering was at a low level as well. Since the number of layers in each graphene platelet is low, the intensity of the diffracted beam is also low. Moreover, a peak located at 43.8° can be observed in the composite XRD pattern, which is associated with Cu (111), suggesting the successful formation of the Cu-graphene composite. Figure 3 shows an SEM image of the synthesized Cu–graphene composite. The graphene flakes were distributed on the Cu surface or embedded in the Cu matrix.

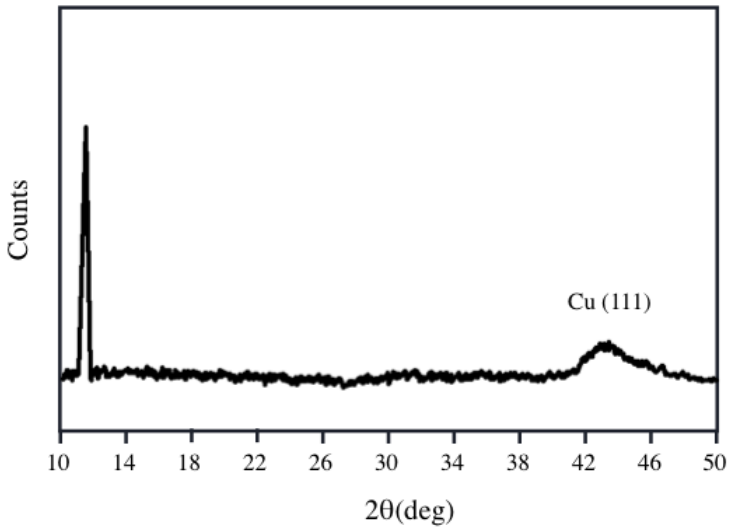

Figure 2. X-ray diffraction pattern of the Cu–graphene composite specimen.

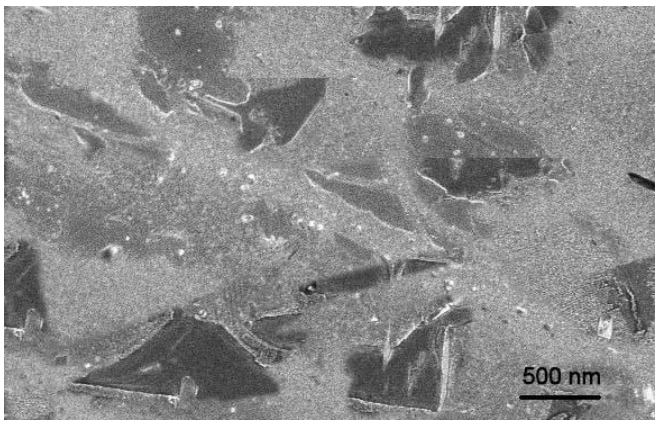

Figure 3. SEM image of Cu–graphene composite specimen.

Figure 4 shows the cyclic voltammograms for cadmium(II) acquired at ITO with and without the modification. At the platinum electrode, a very small peak current can be seen in the potential range between -0.1 V to -0.5 V due to the Cd(II)/Cd(0) redox pair. Moreover, the Cd(II)/Cd(0) redox reaction at the kaolin-modified ITO was easier to recognize. These results show the ability of Cu-graphene to significantly facilitate the preconcentration of cadmium at the ITO surface as well as to improve the sensitivity in detecting cadmium. The performance of the newly developed cadmium-ion sensor is based on the accumulation of cadmium from the aqueous solution onto the surface of the modified electrode [42].

As shown in Figure 5, the behavior of the Cu-graphene-modified ITO film prior to and after the accumulation procedure was studied through electrochemical impedance spectroscopy (EIS). The charge-transfer resistance (R_{tc}) values were determined through the discrepancies in impedance at higher and lower frequencies.

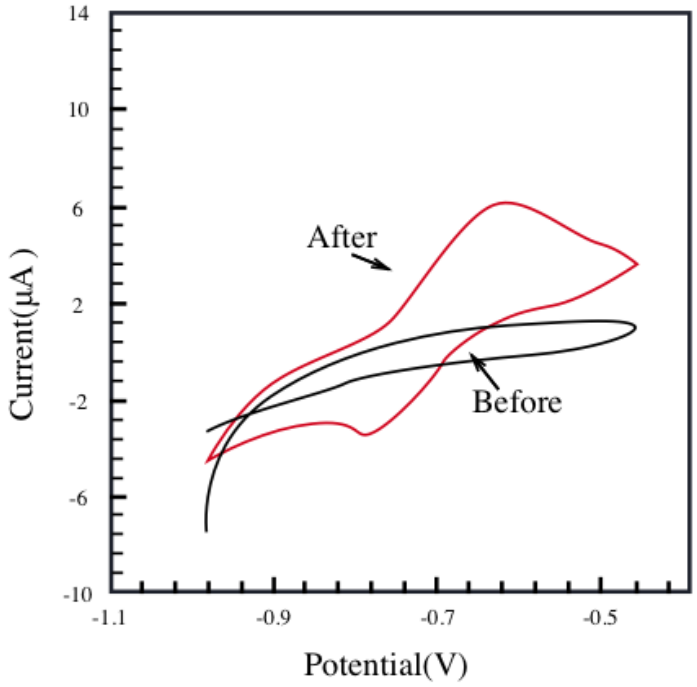

Figure 4. Cyclic voltammograms of the Cu-graphene-modified ITO film prior to any contact with cadmium (II) and after incubation with cadmium (II) for 30 min.

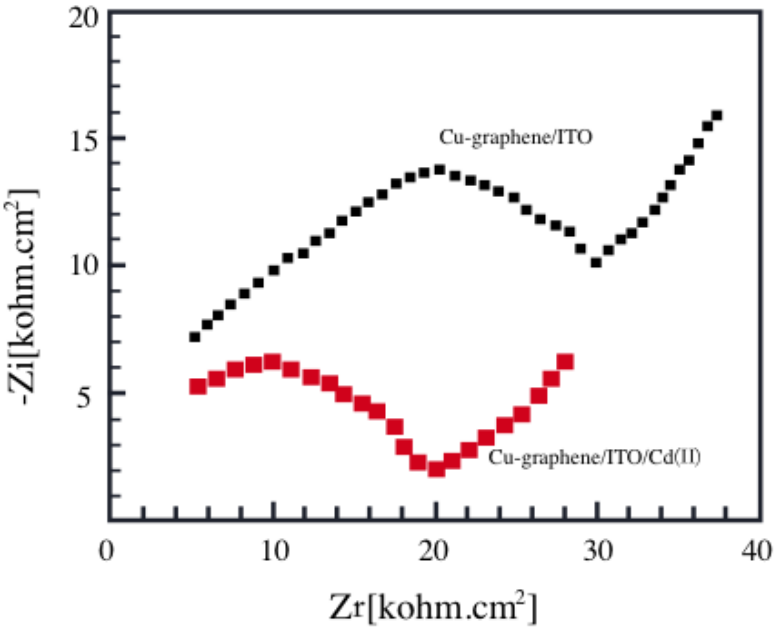

Figure 5. Impedance spectra at 0 V of the CuO-graphene-modified ITO and CuO-graphene/ITO/Cd(II) films.

The dual-layer capacitance (C_{dl}) and the frequency to achieve a maximum imaginary component of the impedance were determined as well. The impedance images were acquired for the frequency domain from 100 kHz to 10 mHz at a potential of 0 V. Table 1 shows the values of R_t,

double-layer capacitance, charge-transfer resistance, and (C_{dl}) from the Nyquist plots. From the impedance data, it can be concluded that there is a decline of the R_t values when there is accumulated cadmium(II). At the same time, the values of the dual-layer capacitance decreased to a minimum value when Cd(II) was present and when the value of (C_{dl}) increases. The improvement of (C_{dl}) was caused by the accumulation of cadmium(II) on the superficial layer of the platinum electrode.

Table 1. Electrical parameters determined from the impedance spectra in 0.2 M KNO_3 for the CuO-graphene/ITO/Cd(II) solution interfaces.

	Re (Ω/cm^2)	Rct (Ω/cm^2)	Cdl (pF/cm^2)
CuO-graphene/ITO	1780	30050	250.5
CuO-graphene/ITO/Cd(II)	720	19970	247.6

Figure 6 demonstrates the change of the anodic peak current versus the accumulation time. When the accumulation time increased, there was an improvement in the peak current, indicating that, prior to adsorption, the accumulation time was positively correlated to the number of Cd(II) ions as well as the peak current. In the following experiments, a preconcentration time of 25 min was applied.

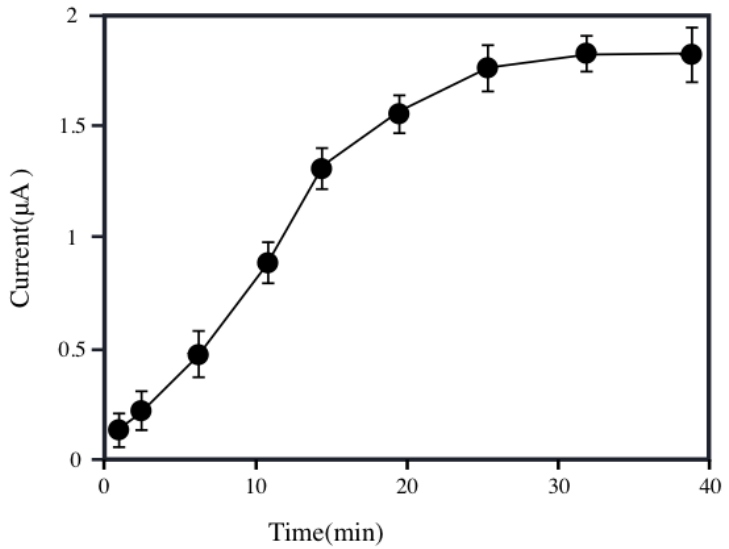

Figure 6. Impact of the accumulation time on the charge transfer of 1.5 μM cadmium(II) in 0.2 M KNO_3.

As revealed in Figure 7, the impact of the pH on the SWV response of ITO after the modification of the CuO-graphene was studied within the pH range of 1.8 to 9.5 in a solution containing 1.5 μM cadmium. The optimal pH range was 4.5-6.0, demonstrating a maximum response when the pH was equal to 5.0. As the intensity of the reduction peak declined, the sensitivity also declined in the acidic solution. This was caused by the tendency of kaolin to gradually dissolve within the acidic solution, losing its adsorption ability. As a result, in the following research, a pH value of 5.0 was utilized.

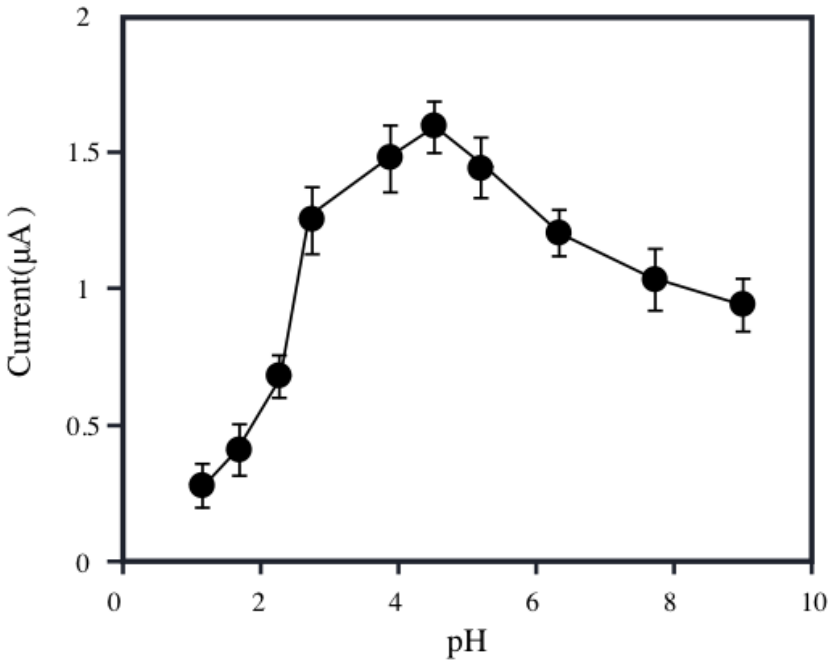

Figure 7. Impact of the pH on the SWV anodic peak for 1.5 μM cadmium(II) in 0.2 M KNO_3.

Figure 8 shows the oxidation peak current of Cd(II) versus the concentration of Cd(II). There is a linear correlation between the peak current of cadmium(II) and its concentration under the optimized conditions, and the correlation can be described by the regression equation of $I(\mu A) = 0.8744Cd(II)_{(\mu M)} + 0.221$ ($r^2 = 0.994$) within the linear dynamic range of 50 nM-8 μM. In the detection of cadmium(II), the detection limit (DL, 3σ) was 12 nM. The relative standard deviation (RSD) for 7 replicate investigations of a solution containing 5.4 μM was 3.31%. According to the National Oceanic and Atmospheric Administration (NOAA), the maximum Cd(II) level allowed in natural waters in the USA is 18 μM. This proposed method can detect Cd(II) at the regulatory level without any further pretreatment of the samples.

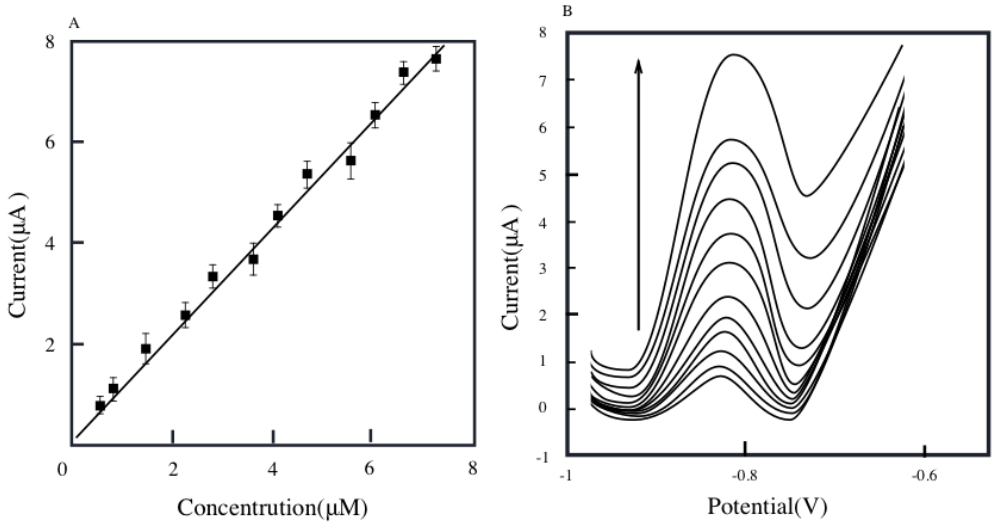

Figure 8. Square-wave voltammograms of cadmium(II) in 0.2 M KNO_3 at the Cu-graphene/ITO film.

The selectivity of this cadmium detection method was assessed through the introduction of other ions into the cadmium specimen solution in the preconcentration procedure. The disturbances of several metal ions while detecting cadmium (II) were also analyzed. The Cu-graphene/ITO film was soaked in a mixture of Cd(II), Cu(II), Ag(I), Pb(II) and Hg(II) (5.0 μM each). The voltammogram shown in Figure 9 demonstrates that the oxidation signal of Cd(II) at −0.85 V was free from any interference under these conditions. The complete separation of the potential peaks indicates that this method is promising for detecting Cd(II) free from any detrimental interference from other heavy metals that are frequently seen. Table 2 shows a comparison of the presented sensor with other cadmium(II) sensors.

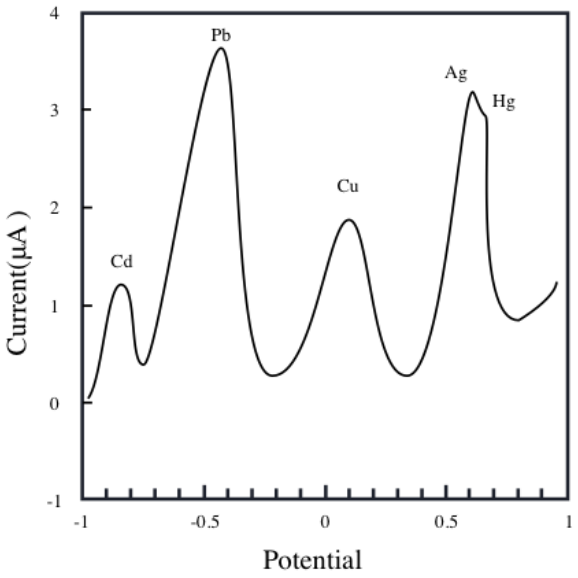

Figure 9. Cyclic voltammogram after exposure to a solution containing Cd(II), Ag(I), Cu(II), Hg(II), and Pb(II).

Table 2. Contrast of the presented electrochemical cadmium (II) sensor with other developed sensors.

Electrode	Detection species	Linear detection range (μM)	Limit of detection (μM)	Reference
Amino-functionalized porous Si nanowires	Cd^{2+}	0.1-10	0.03	[43]
1,9-nonanedithiol/Au	Cd^{2+}	0.01-0.1	—	[44]
Kaolin/Pt	Cd^{2+}	0.09-83	5.4	[45]
Cu-graphene	Cd^{2+}	0.05-8	0.012	This work

4. CONCLUSION

Composite films of Cu-graphene were prepared by electrochemical deposition from an electrolytic solution of $CuSO_4$ containing a GO suspension and further reduction under hydrogen. Square-wave voltammetry was performed for the determination of cadmium(II) at the Cu-

graphene/ITO film. The proposed cadmium(II) sensor exhibited a linear detection range between 0.05 and 8 μM with a low detection limit of 0.012 μM. Moreover, the proposed cadmium(II) sensor also showed good selectivity.

ACKNOWLEDGEMENT
The study is funded by the China Scholarship Fund； Science and Technology Plan Program of Bingtuan(2016AG014)

References

1. F. Barbosa, F. Krug and É. Lima, *Spectrochimica Acta Part B Atomic Spectroscopy*, 54 (1999) 1155.
2. M. Mhammedi, M. Achak and A. Chtaini, *J. Hazard. Mater.*, 161 (2009) 55.
3. E. And and M. Freund, *Journal of the American Chemical Society*, 123 (2001) 3383.
4. M. Prathap, B. Thakur, S. Sawant and R. Srivastava, *Colloids & Surfaces B Biointerfaces*, 89 (2011) 108.
5. M. Ganjali, B. Larijani and E. Pourbasheer, *Int. J. Electrochem. Sci*, 11 (2016) 2119.
6. H. Karimi-Maleh, A. Shojaei, K. Tabatabaeian, F. Karimi, S. Shakeri and R. Moradi, *Biosensors and Bioelectronics*, 86 (2016) 879.
7. J. Wang, D. Thomas and A. Chen, *Anal. Chem.*, 80 (2008) 997.
8. T. Alizadeh, M. Ganjali, M. Akhoundian and P. Norouzi, *Microchim. Acta.*, 183 (2016) 1123.
9. Y. Borghei, M. Hosseini, M. Dadmehr, S. Hosseinkhani, M. Ganjali and R. Sheikhnejad, *Anal. Chim. Acta.*, 904 (2016) 92.
10. S. Cheraghi, M. Taher, H. Karimi-Maleh and R. Moradi, *Journal of The Electrochemical Society*, 164 (2017) B60.
11. R. Ahmad, N. Tripathy, Y. Hahn, A. Umar, A. Ibrahim and S. Kim, *Dalton Transactions*, 44 (2015) 12488.
12. C. Sun, W. Cheng, T. Hsu, C. Chang, J. Chang and J. Zen, *Electrochemistry Communications*, 30 (2013) 91.
13. Y. Z, L. H, Z. X, L. N, T. W, Z. X and Z. L, *Biosensors & Bioelectronics*, 75 (2015) 161.
14. K. Huo, Y. Li, R. Chen, B. Gao, C. Peng, W. Zhang, L. Hu, X. Zhang and P. Chu, *Chempluschem*, 80 (2015) 576.
15. V. Arabali, M. Ebrahimi, M. Abbasghorbani, V. Gupta, M. Farsi, M. Ganjali and F. Karimi, *Journal of Molecular Liquids*, 213 (2016) 312.
16. H. Karimi-Maleh, F. Amini, A. Akbari and M. Shojaei, *Journal of Colloid and Interface Science*, 495 (2017) 61.
17. M. Sheikhshoaie, H. Karimi-Maleh, I. Sheikhshoaie and M. Ranjbar, *Journal of Molecular Liquids*, 229 (2017) 489.
18. C. Zhu, G. Yang, H. Li, D. Du and Y. Lin, *Anal. Chem.*, 87 (2015) 230.
19. B. Yuan, C. Xu, D. Deng, Y. Xing, L. Liu, H. Pang and D. Zhang, *Electrochimica Acta*, 88 (2013) 708.
20. N. Promphet, P. Rattanarat, R. Rangkupan, O. Chailapakul and N. Rodthongkum, *Sensors & Actuators B Chemical*, 207 (2015) 526.
21. D. Zhai, B. Liu, Y. Shi, L. Pan, Y. Wang, W. Li, R. Zhang and G. Yu, *Acs Nano*, 7 (2013) 3540.
22. M. Prathap, T. Pandiyan and R. Srivastava, *Journal of Polymer Research*, 20 (2013) 1.
23. J. Luo, S. Jiang, H. Zhang, J. Jiang and X. Liu, *Anal. Chim. Acta.*, 709 (2012) 47.
24. M. Song, S. Lee, J. Kim and D. Lim, *Journal of the Electrochemical Society*, 160 (2013) B43.

25. R. Pandey and V. Lakshminarayanan, *J. Phys. Chem.C*, 113 (2009) 21596.
26. W. Zheng, S. Jones, X. Hong and S. Tsang, *Rsc Advances*, 4 (2014) 47488.
27. A. Athawale, S. Bhagwat and P. Katre, *Sensors & Actuators B Chemical*, 114 (2006) 263.
28. J. Han, L. Wang and R. Guo, *Journal of Materials Chemistry*, 22 (2012) 5932.
29. G. Wu, Z. Chen, F. Garzon and P. Zelenay, *Ecs Transactions*, 16 (2008)
30. M. Freitag, M. Steiner, Y. Martin, V. Perebeinos, Z. Chen, J. Tsang and P. Avouris, *Nano Letters*, 9 (2009) 1883.
31. F. Xia, D. Farmer, Y. Lin and P. Avouris, *Nano Letters*, 10 (2010) 715.
32. G. Ko, H. Kim, J. Ahn, Y. Park, K. Lee and J. Kim, *Current Applied Physics*, 10 (2010) 1002.
33. H. Yoon, D. Jun, J.H. Yang, Z. Zhou, S. Yang and M. Cheng, *Sensors & Actuators B Chemical*, 157 (2011) 310.
34. T. Kuila, S. Bose, P. Khanra, A.K. Mishra, N. Kim and J. Lee, *Biosensors & Bioelectronics*, 26 (2011) 4637.
35. M. Pumera, A. Ambrosi, A. Bonanni, E. Chng and H. Poh, *Trac Trends in Analytical Chemistry*, 29 (2010) 954.
36. Y. Shao, J. Wang, H. Wu, J. Liu, I. Aksay and Y. Lin, *Electroanalysis*, 22 (2010) 1027.
37. C. Berger, Z. Song, T. Li, X. Li, A. Ogbazghi, R. Feng, Z. Dai, A. Marchenkov, E. Conrad and P. First, *Journal of Physical Chemistry B*, 108 (2004) 19912.
38. M. Liang and L. Zhi, *Journal of Materials Chemistry*, 19 (2009) 5871.
39. G. Wang, X. Shen, J. Yao and J. Park, *Carbon*, 47 (2009) 2049.
40. J. Yoo, K. Balakrishnan, J. Huang, V. Meunier, B. Sumpter, A. Srivastava, M. Conway, A. Reddy, J. Yu and R. Vajtai, *Nano Letters*, 11 (2011) 1423.
41. L. Wang, K. Lee, Y. Sun, M. Lucking, Z. Chen, J. Zhao and S. Zhang, 3 (2009) 2995.
42. M. Mhammedi, M. Achak, M. Hbid, M. Bakasse, T. Hbid and A. Chtaini, *J. Hazard. Mater.*, 170 (2009) 590.
43. Z. Guo, M. Seol, C. Gao, M. Kim, J. Ahn, Y. Choi and X. Huang, *Electrochimica Acta*, 211 (2016) 998.
44. E. Malel, J.K. Sinha, I. Zawisza, G. Wittstock and D. Mandler, *Electrochimica Acta*, 53 (2008) 6753.
45. M. Mhammedi, M. Achak, M. Hbid, M. Bakasse, T. Hbid and A. Chtaini, *J. Hazard. Mater.*, 170 (2009) 590.

© 2017 The Authors. Published by ESG (www.electrochemsci.org). This article is an open access article distributed under the terms and conditions of the Creative Commons Attribution license (http://creativecommons.org/licenses/by/4.0/).